CONF-880896--2

Abstract of invited talk to be presented at the Symposium on Heavy-Ion Reaction Dynamics in Tandem Energy Region, Hitachi, Japah, Aug. 1-3, 1988

CONF-880896--2

DE88 015286

ANGULAR MOMENTUM EFFECTS IN SUBBARRIER FUSION

M. L. HALBERT, J. R. BEENE, D. C. HENSLEY

Oak Ridge National Laboratory,† Oak Ridge, Tennessee 37831

K. HONKANEN,+ T. M. SEMKOW,* V. ABENANTE, D. G. SARANTITES, and Z. LI++

*Washington University,** St. Louis, Missouri 63130*

ABSTRACT

Angular-momentum distributions σ_L for the compound nucleus ^{164}Yb were deduced from measurements of γ-ray multiplicity for all significant evaporation residues from fusion of ^{64}Ni and ^{100}Mo at and below the Coulomb barrier. The excitation functions can be reproduced with coupled-channels calculations only if additional coupling beyond the known inelastic strengths is included. Even with this augmented coupling, however, at the lowest bombarding energies the experimental σ_L extend to higher L values than the predictions. Single-barrier penetration models for a potential with an energy-dependent depth and shape fitted to the excitation function likewise underestimate the role of high-L partial waves. Somewhat better success is achieved with models in which fission is allowed to occur at distances comparable with or even larger than the Coulomb barrier radius.

---

†Operated by Martin Marietta Energy Systems, Inc. under contract DE-AC05-84OR21400 with the U.S. Department of Energy.

+Deceased March 1987.

*Present address: Wadsworth Center for Laboratories and Research, Corning Tower, Albany, NY 12201.

++Permanent address: Physics Division, Institute of Atomic Energy, Beijing, People's Republic of China.

**Work supported by U.S.D.O.E. under contract DE-AS02-76ER04052.

"The submitted manuscript has been authored by a contractor of the U.S. Government under contract No. DE-AC05-84OR21400. Accordingly, the U.S. Government retains a nonexclusive, royalty-free license to publish or reproduce the published form of this contribution, or allow others to do so, for U.S. Government purposes."

MASTER

DISTRIBUTION OF THIS DOCUMENT IS UNLIMITED

7/14/88

ANGULAR MOMENTUM EFFECTS IN SUBBARRIER FUSION

M. L. HALBERT, J. R. BEENE, D. C. HENSLEY
Oak Ridge National Laboratory,† Oak Ridge, Tennessee 37831

K. HONKANEN,+ T. M. SEMKOW,* V. ABENANTE, D. G. SARANTITES, and Z. LI++
*Washington University,** St. Louis, Missouri 63130*

ABSTRACT

Experimental results for cross sections and L distributions in subbarrier fusion of ^{64}Ni + ^{100}Mo are updated. With standard models it seems difficult to reproduce the excitation functions and the L distributions simultaneously, especially at the lowest energies. Models in which the fusion occurs at large distances are more successful.

1. Introduction

Cross sections for fusion of complex nuclei below the Coulomb barrier are well known to be strongly enhanced with respect to predictions of single-barrier penetration models. Various explanations of this phenomenon have been proposed. Measurement of σ_L, the partial-wave distribution in the compound system, would be helpful in distinguishing among the various proposals, but at present such data exist for very few systems.

We have measured cross sections, σ_{fus}, and spin distributions, σ_L, near and below the Coulomb barrier for fusion of ^{64}Ni with ^{100}Mo at the five ^{64}Ni energies given in Table 1. Reaction products corresponding to evaporation of two, three, or four neutrons from the ^{164}Yb compound nucleus were detected by their characteristic γ-ray transitions between low-lying states. These γ rays were registered by six Compton-suppressed Ge detectors which replaced six of the pentagonal NaI units of the Spin Spectrometer, a 72-segment shell of NaI approximating a hollow sphere around the target[1].

---

†Operated by Martin Marietta Energy Systems, Inc. under contract DE-AC05-84OR21400 with the U.S. Department of Energy.
+Deceased March 1987.
*Present address: Wadsworth Center for Laboratories and Research, Corning Tower, Albany, NY 12201.
++Permanent address: Physics Division, Institute of Atomic Energy, Beijing, People's Republic of China.
**Work supported by U.S.D.O.E. under contract DE-AS02-76ER04052.

Table 1. Energies (MeV), cross sections (mb), mean and mean-square values of L weighted by σ_L for ^{64}Ni on ^{100}Mo. E_{beam} is the energy of the beam from the accelerator. E_{cm} is the mean center-of-mass energy weighted according to the variation of yield with energy. The cross sections have uncertainties of about ±15%. The uncertainties in moments of L are probably $\lesssim$10%.

E_{beam}	E_{cm}	σ_{2n}	σ_{3n}	σ_{4n}	$\sigma_{\alpha 2n}$	σ_{fus}	$\langle L \rangle$	$\langle L^2 \rangle$
210.0	127.8	0.26	<0.07	-	-	0.27[a]	16.9	336
215.0	130.1	1.43	1.12	-	-	2.69	19.0	436
220.0	132.8	3.26	5.09	-	-	8.9	21.1	542
225.0	135.5	6.3	16.7	0.9	-	25.6	22.9	633
235.1	141.7	11.0	43.1	18.1	2.3	81.6	28.2	956

[a]Upper limit = 0.34

The unfolding of the Spin Spectrometer data provided intensity maps as a function of excitation energy and γ-ray multiplicity in coincidence with the lowest 2+ → 0+ γ ray in ^{162}Yb or ^{160}Yb, or with the 17/2+ → 13/2+ γ ray in ^{161}Yb; these nuclei are the residuals after 2n, 4n, or 3n evaporation, respectively. Since all the residual nuclei are good rotors, their deexcitation γ rays are mainly stretched E2. The multiplicity coordinate can thus be transformed with small uncertainty to angular momentum of the residual nucleus prior to emission of the γ cascade. The small amount of angular momentum carried off by neutron evaporation can be accounted for with the help of statistical model calculations, and thus the partial-wave distribution in the compound nucleus can be constructed. Details of this procedure and examples of data have been reported earlier [2,3]. Table 1 lists the first and second moments of L (mean and mean-square values of L weighted by the σ_L deduced from experiment).

The fusion cross sections shown in Table 1 and Fig. 1 were obtained by summing the yields of all observed reaction products together with an allowance of 5-10% for channels too weak to be positively identified[2]. The absolute normalization is based on the Coulomb-excitation yield prominent in the Ge spectra, using the cross section predicted by coupled-channels calculations[4]. This normalization agreed satisfactorily (within 12%) with one based on the integrated beam current, the measured target thickness, and the measured Ge efficiencies. The fusion cross sections in Table 1 are 5 to 15% larger than those reported earlier[2,3]

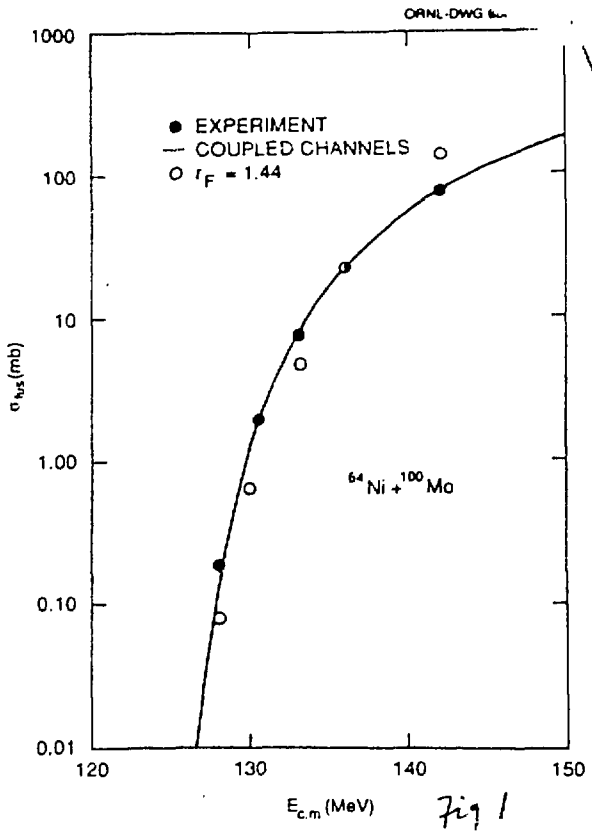

Fig. 1. Excitation function for ^{64}Ni + ^{100}Mo fusion. The experimental data are shown by the full points. The open points are the result of a calculation similar to that of Ref. 19 in which the imaginary potential for fusion is given a sharp cutoff at r_F = 1.44 fm. The curve shows the prediction of a coupled-channels calculation with five inelastic and two transfer couplings. The potential was a Woods-Saxon well with r_0 = 1.0873, V_0 = 108.3, a_V = .707.

because of improvements in our knowledge of the ^{161}Yb decay scheme. Gaardhøje's measurements have shown[5] (and we have confirmed with the ^{16}O + ^{142}Sm reaction) that the lowest 9/2- level decays about 70% of the time by a branch we had not previously taken into account.

In our previous analyses of these data[2,3], we encountered difficulty in simultaneously reproducing the experimental excitation function and the σ_L distributions with various theories: the experimental spin distributions included higher partial waves than the models predicted. These differences in σ_L persisted even when the parameters of the models were adjusted to fit the fusion cross section[3]. A similar problem has been found by others[6]. We believe, along with Vandenbosch et al.[7], that the spin distributions provide significant information beyond that provided by excitation functions alone. We report here further investigations using several models rooted in traditional reaction theory in an effort to isolate the features that determine the spin distributions.

Elastic scattering data for ^{64}Ni + ^{100}Mo do not exist, so we have taken as our starting point a folding-model potential based on the M3Y interaction[8,9]. The calculations were actually done with a Woods-Saxon

parametrization[9] (V_o = 178.3 MeV, r_V = 1.08727, a_V = .707 fm) which represents the folded potential very accurately near the top of the barrier. The barrier height, V_B, for this potential is 138.7 MeV, occurring when the nuclear centers are separated by R_B = 11.41 fm = 1.32 ($64^{1/3}$ + $100^{1/3}$) fm.

2. Coupled-channels calculations

It has been shown that coupling to inelastic channels[10] or transfer channels[11] has the effect of splitting the Coulomb barrier and shifting some barriers to lower energy. This can enhance σ_{fus} by orders of magnitude. Another important effect is an increase of the contribution of higher partial waves. Calculations with exact programs such as Ptolemy[12] are time consuming and difficult to carry out with sufficient accuracy well below the barrier. In the program CCFUS, Dasso and Landowne[13] have provided a fast, approximate method for coupled-channels calculations. We have used CCFUS with inelastic couplings of five excited states to the ground state; the β_λ were taken from the literature[14]. The experimental cross sections and L distributions can be reproduced reasonably well at E_{CM} = 135.5 and 141.7 MeV. At lower energies the predicted cross sections and moments of L are smaller than the experimental values.

We have found that we can match σ_{fus} over the whole range of energies by increasing the coupling strengths: multiplying all β_λ input to CCFUS by 1.5 gave a good representation of the experimental excitation function[3]. It was necessary to reduce V_o from 178.3 to 133.3 MeV to achieve those fits. However, $\langle L \rangle$ and $\langle L^2 \rangle$ at low E_{CM} remained much too small. We have now tried retaining the original β_λ and supplying extra coupling by adding one or two transfer channels,[11] empirically adjusting their strengths and Q values to fit σ_{fus} vs E_{CM}. This was done even though we have not seen any significant yield of transfer products in our Ge spectra. The required coupling strengths appear quite large, F = 9 MeV each for a state at Q = -2 MeV and at Q = -10 MeV. In making these fits, we reduced V_o from 178.3 to 108.3 MeV. The L = 0 barrier with this potential is 143.9 MeV and R_B = 10.92 fm. The calculated results, shown by the full lines in Fig. 1 for σ_{fus} and Fig. 2 for $\langle L \rangle$ and $\langle L^2 \rangle$, are extremely

similar to the 1.5 β_λ calculations[3]. Again, the predicted moments for the low bombarding energies fall well short of experiment.

One may ask whether the need for extra coupling and the failure to match the moments of L might be due to approximations in CCFUS. We have compared its predictions with calculations made with Ptolemy.[12] To carry out the Ptolemy calculations in a reasonable time and with sufficient accuracy, we restricted the couplings to no more than three states and the energies to $E_{CM} \geq 132.8$ MeV. We found excellent agreement between Ptolemy and CCFUS if the coupled states are not strongly Coulomb excited or if Coulomb couplings are turned off in both programs. However, the inclusion of both Coulomb and nuclear excitation in the full coupled-channels calculation for a strongly Coulomb-excited state shows a dramatic interference effect which is not reproduced by CCFUS. For example, with coupling only to the 2^+ 0.53-MeV state in ^{100}Mo, at 141.7 MeV Ptolemy gave σ_{fus} = 88, 113, and 47 mb for uncoupled, nuclear-only, and complete calculations, respectively, while CCFUS gave 88, 106, and 93 mb. (A similar result for full vs. nuclear-only calculations was reported in Ref. 15.) The moments of L are also reduced in the full Ptolemy calculations. The differences are less dramatic if more states are coupled. Nevertheless, the failure of CCFUS to reproduce the experimental σ_L distributions cannot be blamed on approximations in CCFUS since the effect of strong

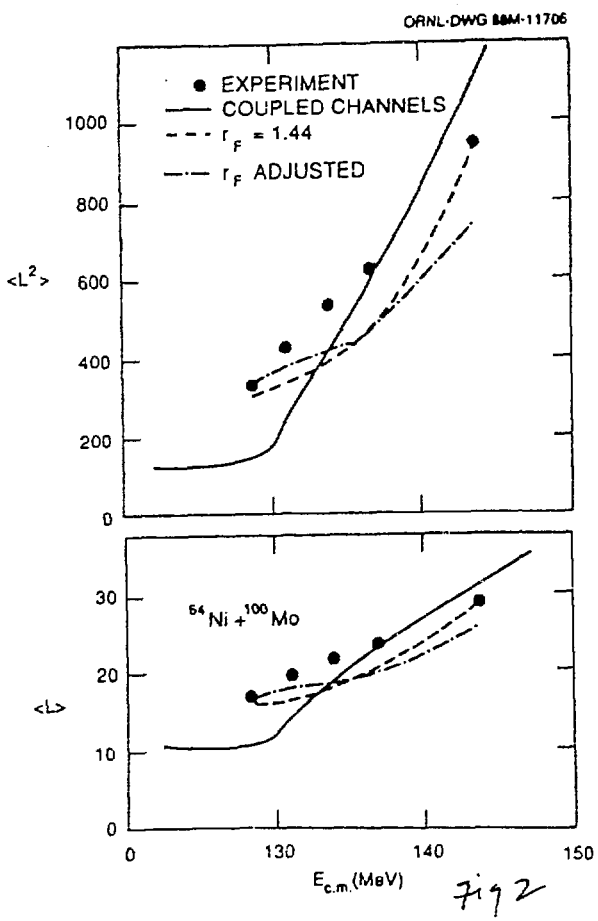

Fig. 2. Bombarding energy dependence of the moments of L. Points are experimental. The dashed curves show calculations similar to those of Ref. 19, in which the cutoff radius parameter r_F was adjusted to fit the experimental σ_{fus}. The full curves are for the coupled-channels calculations of Fig. 1.

Coulomb excitation in Ptolemy is always to reduce, not increase, $\langle L \rangle$ and $\langle L^2 \rangle$.

3. Optical-model approaches

In optical-model theories, the effects of channel coupling are represented by an imaginary potential. This optical-model absorptive well depth, W, should become small as the energy decreases toward the barrier. By means of a dispersion relation, it was shown in Ref. 16 that the real well depth must consequently increase. Optical-model analyses of elastic scattering near the barrier do in fact demonstrate the expected decrease in W and increase in V_0 with decreasing energy[16]. In Ref. 17, it was demonstrated that σ_{fus} obtained from a full coupled-channels calculation could be reproduced by single-channel barrier-penetration calculations in which V_0 was allowed to vary in a way qualitatively consistent with this picture. These calculations, however, fail to reproduce the coupled-channels σ_L distributions unless the shape of the real potential is also adjusted with energy. It was found necessary to increase V_0 and decrease a_V, making the barrier thinner, to match σ_{fus} and σ_L vs. L simultaneously.

We have applied these ideas to our own data. In Ref. 3 we adjusted V_0 to fit the excitation function. This gave σ_L distributions for which $\langle L \rangle$ was only about half of the experimental values. Following Ref. 17, we have now allowed V_0 and a_V to vary simultaneously. Table 2 lists several V_0, a_V combinations that give cross sections equal to the experimental value at E_{CM} = 130.1, 132.8, and 141.7 MeV. We have also done calculations for the limiting case, a Coulomb potential plus an infinitely deep square well ($a_V = 0$) with its radius adjusted to fit σ_{fus} at each energy. The moments of the L distribution for each potential are given in Table 2. Even for rather extreme choices of V_0 and a_V, the $\langle L \rangle$ and $\langle L^2 \rangle$ are smaller than the experimental values at some energies (see Fig. 3). The success reported in Ref. 17 is not observed here, at least not for $a_V \approx .4$ to .5. On the other hand, at the lowest energies $\langle L \rangle$ and $\langle L^2 \rangle$ are closer to the experimental values than are the coupled-channels results; in the limiting case, the agreement is good. The square-well radius at each energy turns out to be rather large, corresponding to a radius parameter for fusion, r_F, between 1.42 and 1.44 fm.

Table 2. Woods-Saxon potential parameters and barrier-penetration results for $^{64}Ni + ^{100}Mo$. In all cases, the radius parameters for the nuclear and Coulomb potentials were 1.0873 fm and 1.2 fm, respectively.

E_{cm} (MeV)	V_0 (MeV)	a_v (fm)	σ_{fus} (mb)	$\langle L \rangle$	$\langle L^2 \rangle$
130.1	178.3	.707	0.000007	9.94	128.7
130.1	1986	.500	2.69	12.36	196.5
130.1	8300	.400	2.70	13.07	219.3
130.1	95000	.300	2.71	13.90	147.3
130.1	13.3×10^6	.200	2.69	14.90	282.4
130.1	∞	0	2.69	16.97	360.3
132.8	178.3	.707	0.0009	10.07	131.9
132.8	1463	.500	8.90	12.80	208.6
132.8	59780	.300	8.90	14.40	263.0
132.8	7.15×10^6	.200	8.90	15.49	302.7
132.8	∞	0	8.90	17.99	400.2
141.7	178.3	.707	86.2	18.56	401.0
141.7	586	.500	81.5	18.75	412.9
141.7	13560	.300	81.6	19.63	455.9
141.7	883000	.200	81.6	20.35	490.4
141.7	4.09×10^{11}	.100	81.8	21.59	550.3
141.7	∞	0		23.8[a]	655.[a]
127.8	∞	0	.27	15.84	317.8
135.5	∞	0	15.6	19.69	470.2

[a]Extrapolated value.

It has traditionally been assumed[18] that the absorptive well for fusion is confined to distances similar to the nuclear half-density radius, corresponding to $r_0 \sim 1.0$ fm, so that fusion occurs only inside the Coulomb barrier. Udagawa, Tamura, and coworkers[19,20] have demonstrated success in fitting fusion cross sections and σ_L distributions with a formalism similar to that of Ref. 17 except that fusion was not confined to small distances. They separate the absorptive potential into a fusion part and a direct part by a sharp[19] or slightly diffuse[20] cutoff at some particular radius adjusted to fit σ_{fus} (and $\sigma_{elastic}$ in Ref. 20). This radius usually turns out to correspond to a rather large radius parameter, $r_F \sim 1.4$ fm, which means that fusion is occurring under the barrier or even outside it. Although the physical justification for the assumptions of Refs. 19 and 20 is not clear at present, we have made similar direct-reaction calculations for $^{64}Ni + ^{100}Mo$ by means of program FRESCO[21]. With a fixed $r_F = 1.44$ fm, we obtain a reasonable representation of the excitation function, as shown by the open points in Fig. 1. The moments of L are shown by the dashed

curve in Fig. 2. If we adjust r_F at each energy to fit the excitation function, as was done in Ref. 20, r_F varies slightly with energy (1.40 to 1.455 fm). The corresponding moments of L are shown by the dash-dot curve in Fig. 2. Below the barrier, these results are nearly the same as for the infinite square well (Table 2). This is not surprising since in both cases the radius of the sharp-edged absorptive region was adjusted to match the same σ_{fus} data.

4. Empirical barrier distributions

Stelson has taken an empirical approach, asking what distribution of barriers can reproduce observed excitation functions for a large number of systems[22,23]. He has found that uniform rectangular distributions (or slight modifications of a uniform distribution) can reproduce nearly all the experimental data by adjustment of two parameters, B_m and B_t, that specify the center and width of the rectangular distribution. A third parameter describing the "modulation" of the cross section is usually needed to enhance the lowest-energy region. Stelson has found[23] that an excellent representation of our excitation function can be obtained with a mean barrier, B_m, of 142.2 MeV, a half-width $B_m - \bar{B}_t = 13.7$ MeV, and a Gaussian modulation with $\sigma_B = 1.6$ MeV. The σ_L distributions reproduce the experimental ones reasonably well at high energies,

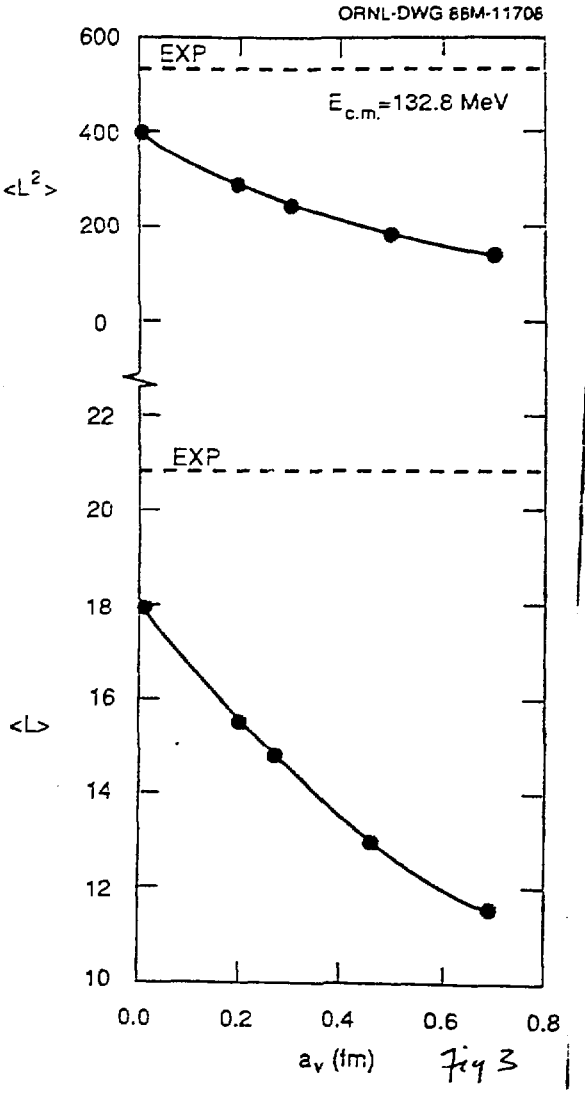

Fig. 3. Moments of L for ^{64}Ni + ^{100}Mo fusion at E_{CM} = 132.8 MeV. The experimental values are shown by the dashed lines. The points are results of barrier-penetration calculations as a function of the diffuseness, a_v, for the potentials listed in Table 2. For each a_v choice, V_0 was adjusted to match the experimental σ_{fus}. The point for a_v = 0 is the limiting case of an infinite square well.

but, as usual, not at the lowest energies. Allowing the barrier distance, R_B, to increase by several fm at low energy improves the σ_L agreement[23]).

5. Summary and remarks

Neither the approximate coupled-channels calculations nor the barrier-penetration model of Ref. 17 appear able to reproduce the excitation function and the σ_L distribution simultaneously. One possible interpretation for this failure, especially in view of the comparative success of the sharp cutoff approximation of Ref. 19, is that fusion of nearly symmetric systems occurs at internuclear separations well outside the top of the L = 0 barrier. The model of Udagawa et al.[19]) does not provide information concerning the physical phenomena that might be responsible for fusion at large distances. The failure of the coupled-channels calculations indicates that the answer lies outside the degrees of freedom explicitly included in those calculations. Perhaps calculations carried out from a more macroscopic point of view, such as those of Iwamoto and Harada[24]), contain part of the answer since their results indicate that neck formation leading to fusion can occur well outside the unperturbed barrier. We should also mention that Stelson has shown[22]) that the parameters deduced for the empirical barrier distributions can be related, via arguments employing the summed single-neutron potentials, to sudden opening of a window for neutron flow between the reactants. The nuclear separation at which such flow would commence is similar to that found from the empirical adjustments reported here and in Ref. 19.

Despite these suggestive results, we feel it is premature to claim that our data identify fusion at large separation as a clear explanation of the discrepancies we have found. We reiterate a point made by Vandenbosch[7]): it may be inaccurate to assume that during the course of a fusion reaction the reduced mass and the barrier radius are (a) invariant and (b) independent of L. These questions have not been specifically addressed in models of fusion as far as we know.

References

1) M. Jääskeläinen et al., Nucl. Instrum. Methods 204 (1983) 385.
2) M. L. Halbert et al., Symposium on the Many Facets of Heavy-Ion Fusion Reactions, ANL-PHY-86-1, 511 (1986).
3) M. L. Halbert et al., Frontiers of Heavy-Ion Physics, ed. N. Cindro, W. Greiner, and R. Caplar (World Scientific 1987), p. 323.
4) J. Raynal, program ECIS.
5) J. J. Gaardhøje, thesis, University of Copenhagen (1980).
6) T. Murakami et al., Phys. Rev. C 34 (1986) 1353.
7) R. Vandenbosch et al., Phys. Rev. Lett. 57 (1986) 1499.
8) G. R. Satchler and W. G. Love, Phys. Reports 55, (1979) 183.
9) G. R. Satchler, private communication.
10) C. H. Dasso et al., Nucl. Phys. A405 (1983) 381.
11) R. A. Broglia et al., Phys. Lett. 133B (1983) 34.
12) M. J. Rhoades-Brown et al., Phys. Rev. C 21 (1980) 2417.
13) C. H. Dasso and S. Landowne, Phys. Lett. B183 (1987) 141; Computer Phys. Comm. 46 (1987) 187.
14) For ^{64}Ni: M. L. Halbert, Nuclear Data Sheets 28 (1979) 179; E. Fabrici et al., Phys. Rev. C 21 (1980) 844; J. Albinski et al., Nucl. Phys. A445 (1985) 477. For ^{100}Mo: J. Barrette et al., Phys. Rev. C 6 (1972) 1339; P. Paradis et al., Phys. Rev. C14 (1976) 835; H. Bohn et al., Z. Phys. A274 (1975) 327; M. Pignanelli et al., Phys. Rev. C 29 (1984) 434; S. J. Burger and G. Heymann, Nucl. Phys. A243 (1975) 461.
15) S. Landowne and S. C. Pieper, Phys. Rev. C 29 (1984) 1352.
16) M. A. Nagarajan et al., Phys. Rev. Lett. 54 (1985) 1136; C. Mahaux et al., Nucl. Phys. A449 (1986) 354.
17) G. R. Satchler et al., Annals of Physics 178 (1987) 110.
18) S. Steadman and M. J. Rhoades-Brown, Ann. Rev. Nucl. Sci. 36 (1986) 649, especially p. 667.
19) T. Udagawa et al., Phys. Rev. C 32 (1985) 1922; B. T. Kim et al., Phys. Rev. C 33 (1986) 370.
20) T. Udagawa, Legnaro symposium "Heavy Ion Interactions Around the Coulomb Barrier," June 1-4, 1988.
21) I. J. Thompson, Computer Phys. Comm. (in press).
22) P. H. Stelson, Phys. Lett. 205B (1988) 190.
23) P. H. Stelson, private communication.
24) A. Iwamoto and K. Harada, Z. Phys. A326 (1987) 201.

"The submitted manuscript has been authored by a contractor of the U.S. Government under contract No. DE-AC05-84OR21400. Accordingly, the U.S. Government retains a nonexclusive, royalty-free license to publish or reproduce the published form of this contribution, or allow others to do so, for U.S. Government purposes."

DISCLAIMER

This report was prepared as an account of work sponsored by an agency of the United States Government. Neither the United States Government nor any agency thereof, nor any of their employees, makes any warranty, express or implied, or assumes any legal liability or responsibility for the accuracy, completeness, or usefulness of any information, apparatus, product, or process disclosed, or represents that its use would not infringe privately owned rights. Reference herein to any specific commercial product, process, or service by trade name, trademark, manufacturer, or otherwise does not necessarily constitute or imply its endorsement, recommendation, or favoring by the United States Government or any agency thereof. The views and opinions of authors expressed herein do not necessarily state or reflect those of the United States Government or any agency thereof.